

Titrateable Avidity Reduction Enhances Affinity Discrimination in Mammalian Cellular Selections of Yeast-Displayed Ligands

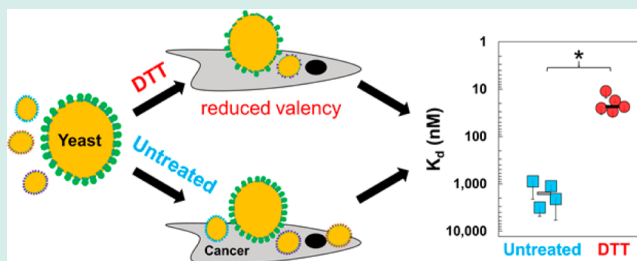
Lawrence A. Stern,[†] Clifford M. Csizmar,[‡] Daniel R. Woldring,[†] Carston R. Wagner,[‡] and Benjamin J. Hackel^{*,†}

[†]Department of Chemical Engineering and Materials Science and [‡]Department of Medicinal Chemistry, University of Minnesota—Twin Cities, Minneapolis, Minnesota 55455, United States

S Supporting Information

ABSTRACT: Yeast surface display selections against mammalian cell monolayers have proven effective in isolating proteins with novel binding activity. Recent advances in this technique allow for the recovery of clones with even micromolar binding affinities. However, no efficient method has been shown for affinity-based selection in this context. This study demonstrates the effectiveness of titrateable avidity reduction using dithiothreitol to achieve this goal. A series of epidermal growth factor receptor binding fibronectin domains with a range of affinities are used to quantitatively identify the number of ligands per yeast cell that yield the strongest selectivity between strong, moderate, and weak affinities. Notably, reduction of ligand display to 3,000–6,000 ligands per yeast cell of a 2 nM binder yields 16-fold better selectivity than that to a 17 nM binder. These lessons are applied to affinity maturation of an EpCAM-binding fibronectin population, yielding an enriched pool of ligands with significantly stronger affinity than that of an analogous pool sorted by standard cellular selection methods. Collectively, this study offers a facile approach for affinity selection of yeast-displayed ligands against full-length cellular targets and demonstrates the effectiveness of this method by generating EpCAM-binding ligands that are promising for further applications.

KEYWORDS: ligand discovery, protein engineering, fibronectin domain, combinatorial library screening



INTRODUCTION

A variety of engineered proteins have proven effective for molecularly targeted therapeutics¹ and diagnostics² for numerous disease states. The ever-growing landscape of clinically relevant cellular biomarkers motivates the continued development of new agents to diagnose and treat newly characterized conditions.

For this demand to be met, several high-throughput methods for selecting engineered proteins with novel binding functionality have been developed. One such method involves the selection of yeast surface-displayed ligands against mammalian cell monolayers,^{3,4} which has been successfully implemented to isolate antibody fragments against brain endothelial cells,⁵ B7–H4,⁶ and androgen-dependent prostate cancer.⁷ Ligands discovered through this method are selected against full-length extracellularly expressed transmembrane proteins, which differs from traditional selection methods using immobilized^{8,9} or fluorescently labeled¹⁰ recombinant extracellular domains. Selections against recombinant extracellular domains can fail to translate to cellular binding for a variety of reasons, including the presence of unstable soluble domains,^{11–14} incorrect post-translational modification,^{15,16} presence of biological or chemical tags,¹⁷ or exposure of epitopes that would not be accessible in the full-length protein. In some instances, results have been reported showing that a subset of clones isolated from selection campaigns using recombinant extracellular domains do not bind the full-length cellular target.^{18,19}

In more extreme instances, ligand selection campaigns relying on selection against recombinant extracellular domains can fail completely. However, as there is no good outlet for this result, these difficulties are seldom reported but nevertheless motivate the use of cellular proteins as targets for ligand selection.

Recent advances in yeast-displayed cell panning allow for the recovery of ligands with even micromolar binding affinities.²⁰ Although such modest affinities can be drastically improved by recursive mutagenesis,^{21–24} an efficient cellular panning method has not yet been demonstrated for discrimination of higher affinity ligands from their weaker counterparts. One alternative method for affinity selection against full-length transmembrane proteins is fluorescence-activated cell sorting (FACS) with detergent-solubilized cell lysates.^{4,25,26} This method utilizes amphiphilic detergent molecules to stabilize the hydrophobic transmembrane domain, allowing these proteins to be used in selection in a concentration-dependent manner. In cell panning, it has been shown that an 8-fold decrease in the target expression of mammalian cells (from $(1.5 \pm 0.6) \times 10^6$ to $(1.9 \pm 0.6) \times 10^5$ targets per cell) drastically decreases the recovery of weaker variants (17 ± 4 nM and micromolar affinity) while still allowing measurable recovery of a high

Received: December 22, 2016

Revised: March 17, 2017

Published: March 21, 2017

affinity (2 ± 2 nM) clone in an epidermal growth factor receptor (EGFR) expressing system.²⁰ This suggests that the avidity between yeast and a mammalian cell is much less requisite on the recovery of stronger binding interactions. However, it is not always easy to generate cell lines with target expression ranging over several orders of magnitude. Further, expression variation cannot be achieved in cases where the biomarker's identity is not known or where the target cells are not stably cultured (e.g., patient biopsy samples). The same study showed that decreasing the ligand expression of the yeast cell over a 3.5-fold range did not adversely affect recovery of either the 2 ± 2 or 17 ± 4 nM affinity variants. However, the weakest protein expression tested was near 10,000 ligands per yeast cell, which still has high avidity potential.

This study aims to determine if a further decrease in yeast valency can yield affinity discrimination in yeast-displayed cell panning selections. As ligands are tethered to the yeast surface by two disulfide linkages between yeast mating proteins agglutinin 1 (Aga1p) and agglutinin 2 (Aga2p), we demonstrate that controlled avidity reduction is achievable by titration with dithiothreitol (DTT). In a model system, we select mixtures of fibronectin domain clones with low and mid nanomolar and micromolar affinities for EGFR²⁰ against cancer cell monolayers expressing $(1.5 \pm 0.6) \times 10^6$ EGFR per cell to optimize the level of avidity reduction for preferential recovery of stronger binding interactions. Using this system, we show that a reduction from 8,000 to 3,000–6,000 ligands/cell is enough to observe a 16-fold enrichment advantage of a 2 nM binder relative to a 17 nM binder. However, a drastic decrease in avidity to 400 ligands/cell abolishes the ability to select, returning essentially the starting mixture composition. We then apply the lessons learned from this model system to the discovery and affinity selection of novel hydrophilic fibronectin domains engineered to bind epithelial cell adhesion molecule (EpCAM).

RESULTS AND DISCUSSION

Yeast surface display selections against mammalian cell monolayers have shown success in the past, but their inability to preferentially select for high affinity ligands has been demonstrated. The lead published scFvs isolated using this method have affinities of 82 ± 15 nM for rat brain endothelial (RBE4) cells⁵ and 27 ± 16 nM (determined multivalently) for androgen-dependent prostate cancer cells.⁷ In both studies, numerous isolated scFvs required dimerization to assess binding character, suggesting clones with weaker affinities were isolated. Moreover, our aforementioned model system experiment yielded minimal differentiation of 2 ± 2 relative to 17 ± 4 nM affinities.²⁰ Although functional for in vitro studies, preferential selection of stronger binders can aid in vivo imaging and therapeutic applications.²⁷ We sought to solve this by shifting from avidity- to affinity-driven interactions by decreasing yeast-displayed ligand expression in a controlled manner.

Effect of DTT Concentration on Yeast-Displayed Ligand Expression. To determine the parameters to effectively tune ligand display levels, yeast expressing the EGFR-binding fibronectin domain E6.2.6' in pCT-40 vector were subjected to 0–20 mM DTT concentrations for 20 min to reduce the Aga1p-Aga2p disulfide tether. Ligand display levels were assessed by flow cytometry analysis of untreated and treated yeast by labeling the C-terminal MYC tag and were found to decrease in a titratable way with increasing DTT concentration (Figure 1A). Retention of 96 ± 17 , 40 ± 19 , and $15 \pm 14\%$ of ligands was observed for 0.5, 5, and 10 mM DTT, respectively.

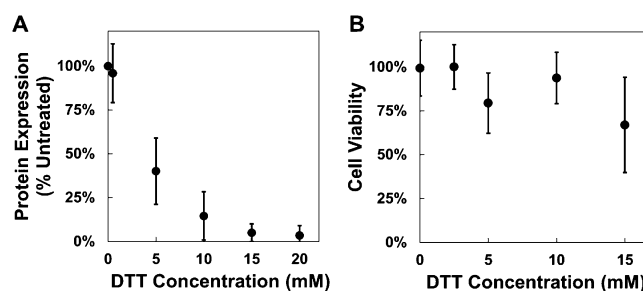


Figure 1. Effect of DTT digestion on ligand display and yeast cell viability. Yeast displaying EGFR-binding fibronectin clone E6.2.6' were subjected to DTT digestion at the indicated concentrations. (A) Relative fibronectin expression after DTT digestion was assessed by flow cytometry analysis of untreated and treated yeast by labeling the C-terminal MYC tag. Results are expressed as mean \pm standard deviation of four or five trials. (B) Cell viability of yeast displaying E6.2.6' or mixtures of E6.2.6', E6.2.6' N78S, and E6.2.6' AASV after DTT treatment was assessed by dilution plating and is expressed as mean \pm standard deviation of five trials.

As DTT is able to internalize and potentially reduce proteins essential to biological processes, yeast viability was also assessed by dilution plating prior to and after treatment (Figure 1B). Yeast remained at least $79 \pm 17\%$ viable for DTT concentrations up to 10 mM. Treatment with 15 mM DTT caused a viability decrease to $67 \pm 27\%$ (though this decrease does not meet the typical level for statistical significance relative to the untreated case; $p = 0.08$). This knowledge allows for tuning of the ligand display level to satisfy the selection criteria needed.

Selection of Fibronectin Domains with Reduced Avidity Against EGFR-Expressing Cells. The effect of reduced avidity on cellular selection was first evaluated in an EGFR-expressing model system. Mixtures of yeast displaying previously characterized fibronectin domains with high, mid, and low affinity (2 ± 2 , 17 ± 4 , or >600 nM K_d , respectively²⁰) for EGFR were treated with DTT and selected for binding to EGFR-overexpressing MDA-MB-468 human breast cancer cells (1.5×10^6 EGFR per cell²⁰) (Figure 2). Flow cytometry was used to determine the composition of the starting mixture prior to selection, and the resultant populations returned after cell panning. The starting mixture contained $1.4 \pm 0.1\%$ high affinity (E6.2.6'), $6.8 \pm 1.4\%$ mid affinity (E6.2.6' N78S), and $92 \pm 1.4\%$ low affinity (E6.2.6' AASV) ligand expressing yeast (Figure 2A). Selection from this pool without DTT treatment (8,000 ligands/cell) yields (18 ± 5.8) -fold enrichment of E6.2.6' and (12 ± 2) -fold enrichment of E6.2.6' N78S with strong disenrichment of E6.2.6' AASV (Figure 2B). Although E6.2.6' does significantly outperform E6.2.6' N78S ($p = 0.02$) from an enrichment standpoint, the 1.6-fold selectivity improvement with strong affinity is not enough to expect higher affinity clones to overtake the population in an efficient number of selection rounds. Display reduction to 6,000 ligands/cell (25% decrease) drastically increases affinity discrimination, yielding enrichment of (42 ± 2) -fold for E6.2.6' and 2.7 ± 0.4 for E6.2.6' N78S (Figure 2B), providing (16 ± 3) -fold selectivity between high and mid affinity (Figure 2C). Further reduction to 3,000 ligands/cell (63% decrease) shows a similar result with (33 ± 8) -fold enrichment for E6.2.6' and (2 ± 0.3) -fold enrichment for E6.2.6' N78S (Figure 2B), retaining the (16 ± 5) -fold advantage of high affinity (Figure 2C). Further display reduction to 1,000 ligands/cell reduces selectivity to (5.3 ± 1) -fold. At 400 ligands/cell, the system enters a regime

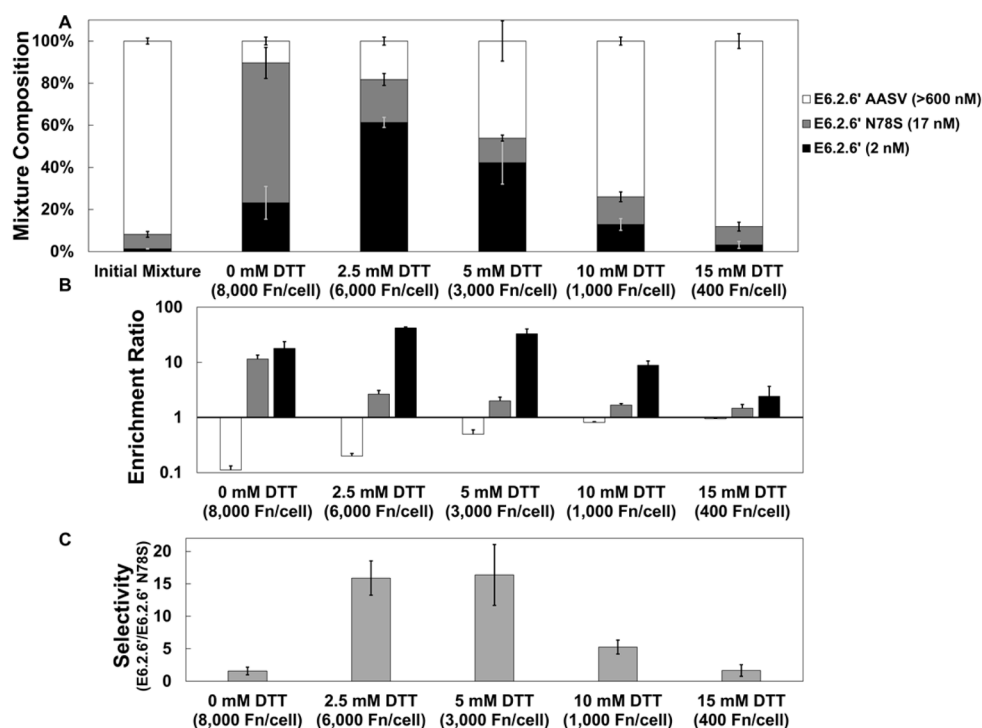


Figure 2. Effect of reduced ligand expression on affinity selection against EGFR-expressing mammalian cells. Yeast displaying fibronectin clones E6.2.6', E6.2.6' N78S, and E6.2.6' AASV (affinities indicated²⁰) were mixed and digested with the indicated amounts of DTT. Following DTT treatment, the ligand expression was quantitated by flow cytometry. DTT-treated yeast were then panned against EGFR-positive MDA-MB-468 monolayers. (A) The mixture composition, (B) enrichment ratio for each clone, and (C) selectivity for E6.2.6' relative to E6.2.6' N78S are indicated as the mean \pm standard deviation of eight selections with the exception of the initial mixture, which is the mean \pm standard deviation of four mixtures.

where the ability to select becomes hindered, yielding a sorted composition that resembles the initial input (Figure 2A). In all cases, E6.2.6' AASV is disenriched relative to the mid and high affinity ligands.

The avidity between yeast and a mammalian cell is important to keep binding interactions intact throughout incubation and to withstand the shear stress associated with washing the monolayer. The weak selectivity between E6.2.6' and E6.2.6' N78S without a reduction in the number of ligands on the yeast surface indicates that, within this affinity range, it is the high avidity between yeast and a mammalian cell that is driving recovery rather than ligand affinity. Reducing the number of ligands to between 3,000 and 6,000 ligands per yeast cell increases the selectivity between these two clones because the diminished number of interactions between a yeast and mammalian cell causes ligand affinity to become more impactful in the ability of yeast to remain bound. Further reduction to 1,000 ligands per yeast cell shows a decrease in selectivity as there is no longer enough avidity to reliably keep many of the yeast bound to the mammalian cell. With extreme reduction to 400 ligands per yeast cell, the avidity between yeast and the mammalian cell is generally not strong enough to keep yeast bound through incubation and washing regardless of affinity, and thus, essentially no selection is observed. These results suggest that although this method of affinity selection can yield coarse affinity discrimination, the level of discrimination is not likely to be as fine as fluorescence-activated cell sorting with soluble target²⁸ or with detergent-solubilized cell lysate²⁵ because the sort stringency of these techniques is tunable by simply drawing a strict sort gate. However, the ability to differentiate a 2 nM interaction from 17 and >600 nM interactions in these

experiments is the first example of affinity discrimination with yeast surface display against mammalian cell monolayers, a selection method that did not previously have any method for affinity discrimination.

Not all ligands display at the same level. It should be noted that, in these experiments, the ligands remaining per cell after DTT treatment, not the concentration of DTT used, is the most important metric for successful selection. In the event that a ligand expresses at a level requiring greater than 10 mM DTT for the necessary level of ligand removal, other reducing agents with less cytotoxicity,²⁹ such as tris(2-carboxyethyl)phosphine (TCEP), should be tested for efficacy and yeast viability.

It should also be emphasized that not all ligands will be compatible with this selection. In particular, disulfide-stabilized ligands such as antibody fragments or cystine knot peptides may exhibit detrimental conformational change due to destabilization from reduction. However, such changes could also serve to reduce functional valency, which could potentially achieve the same goal as Aga1p-Aga2p separation. Thus, the DTT reduction approach could still be used, but DTT titration should be performed while acknowledging that disulfide reduction could impact both the Aga1p-Aga2p bonding and ligand conformation. Alternatively, for a more analogous avidity reduction for use with these ligands to be achieved, digestion with factor Xa protease can be optimized to yield yeast with the appropriate number of ligands per yeast cell. A cut site for factor Xa protease is present in the yeast surface display linker N-terminal to the ligand.

Affinity Maturation of EpCAM-Binding Fibronectin Domains. EpCAM is an attractive cancer target due to its overexpression in many different carcinomas including those of

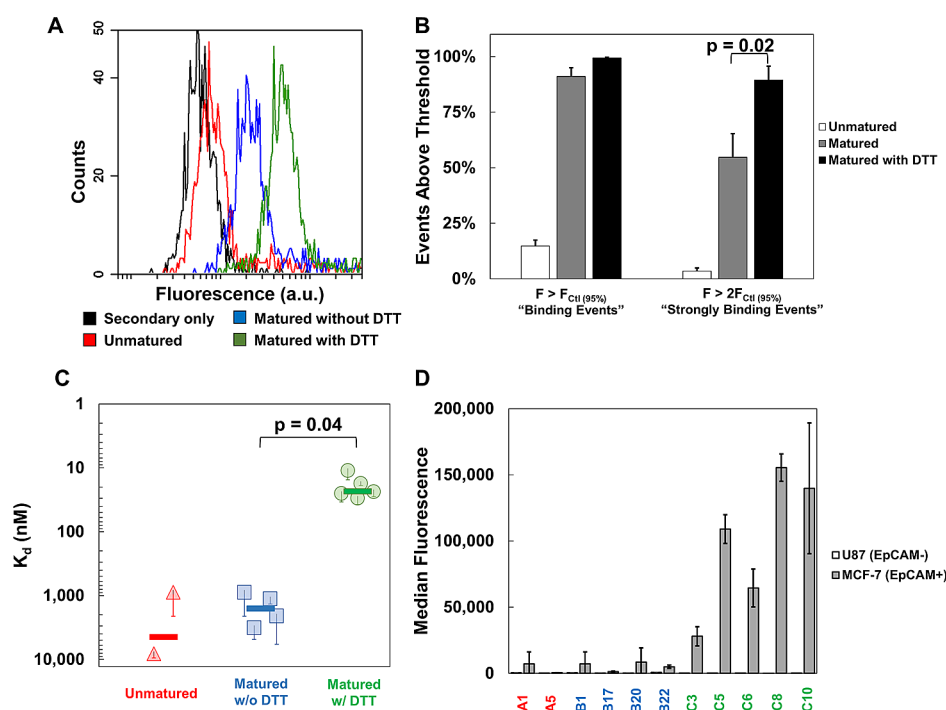


Figure 3. Characterization of EpCAM-binding fibronectin populations and individual clones. (A) Polyclonal populations of soluble EpCAM-binding fibronectin domains were assessed for relative affinity against EpCAM-expressing MCF-7 cells at 10 nM via flow cytometry. (B) Quantitative analysis of the flow cytometry experiments was performed. For this analysis, the percentage of fluorescent events appearing above the 95th percentile (“binding events”) and 2-fold above the 95th percentile (“strongly binding events”) of the negative control were quantified as mean \pm standard error of eight trials. (C) Individual fibronectin clones were produced solubly, and their affinity toward EpCAM-expressing MCF-7 cells was determined by flow cytometry. Affinities are presented as mean \pm standard error of two to five trials (instances where only two trials were performed are presented as mean \pm range). (D) The same soluble fibronectin clones were assessed for binding against EpCAM-negative U87 cells at 100 nM via flow cytometry to determine the specificity of these clones. Clones are named with letters corresponding to the population from which they were isolated: “A” denotes clones isolated from the unmaturing population, “B” denotes clones isolated from the population matured without DTT, and “C” denotes clones isolated from the population matured with DTT. The coloring of clone names further represents their parent population akin to (A) and (C). Median fluorescence intensities are presented as mean \pm standard error of two to five trials (instances where only two trials were performed are presented as mean \pm range). All samples include U87 (EpCAM-negative) data, but most U87 bar (white) are not visible because of their near-zero fluorescence after background correction.

the breast, pancreas, esophagus, colon, and prostate.³⁰ Many ligands have been evolved for EpCAM binding including antibodies and their fragments,³¹ shark vNARs,³² DARPins,^{33,34} and small cyclic peptides.³⁵ Fibronectin domains^{36,37} have never been applied to EpCAM binding but their evolvability for high affinity and specificity, small size, and ease of production and downstream handling could provide an advantage over established ligands.

A population of EpCAM-specific fibronectin domains was selected through a combination of magnetic bead sorting and FACS sorting with a soluble EpCAM extracellular domain and cellular-based selection using MCF-7 and LnCAP cells. Three rounds of mutagenesis and selection were carried out to seek improved affinity. Clones isolated at this stage exhibited only moderate affinity for the soluble EpCAM extracellular domain ($K_d \approx 130$ – 190 nM; Figure S2) and weak binding to EpCAM-expressing human cell lines. Therefore, we sought to isolate higher affinity clones from the population via our avidity reduction approach.

Three populations of EpCAM-binding fibronectin domains are compared: (1) an enriched pool of fibronectins obtained after three rounds of selection with avidity reduction (matured population with DTT), (2) a population from the same round of directed evolution sorted by standard cell panning methods (matured population without DTT), and (3) the population

from the previous round of directed evolution (unmatured population). Soluble fibronectin domains from each population were produced as a polyclonal mixture and tested for binding to EpCAM-positive MCF-7 cells (Figure 3A). For analysis of this data, binding is considered detectable for all events with fluorescence above the 95th percentile of the negative control. Binding is considered strong for events lying 2-fold above the 95th percentile of the negative control (Figure 3B). The unmaturing population contains $15 \pm 3\%$ detectable binding events and $3 \pm 1\%$ strongly binding events. Upon mutagenesis and additional cell panning, the matured population distribution shifts to include more variants with stronger binding to MCF-7 cells with $91 \pm 4\%$ of events detectable and $55 \pm 11\%$ appearing strong. When the mutated population is instead panned using yeast valency reduction with DTT, the resulting variants essentially all bind ($99 \pm 0.2\%$ of events detectable) and are predominantly strong binders ($89 \pm 6\%$). Significantly more strong binders are found in the matured population panned using yeast valency reduction than the matured population panned without DTT treatment ($p = 0.02$). For this difference in affinity to be examined further, individual clones from each population were selected based on differences observed in individual sequences obtained from Sanger sequencing of random clones. A subset of these clones were produced as soluble, monoclonal domains and purified. Affinities of these

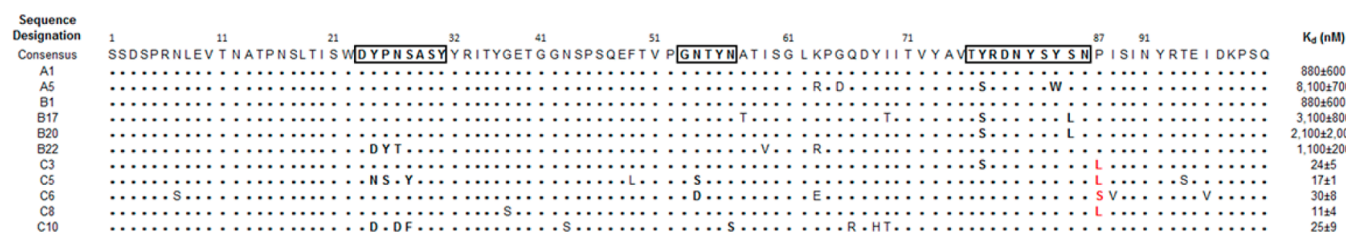


Figure 4. Sequences for EpCAM-binding fibronectin domains, which were compared by sequence alignment. Residues that match consensus are denoted by a •. Engineered loop residues are shown in bold. P87L/S mutation is highlighted in red. Clones are labeled with letters corresponding to the population from which they were isolated: “A” denotes clones isolated from the unmaturation population, “B” denotes clones isolated from the population matured without DTT, and “C” denotes clones isolated from the population matured with DTT.

clones were determined by flow cytometry (Figure 3C). The affinities of clones isolated from the matured population with DTT (median: 24 nM) were significantly higher ($p = 0.04$) than those of clones isolated from the matured population without DTT (median: 1,600 nM). Furthermore, these higher affinity clones are comparable to a commercially available monoclonal antibody known to target EpCAM (clone 9C4) when tested in parallel in a flow cytometry-based cell binding assay (Figure S3). Importantly, none of the tested clones with strong affinities bind appreciably to EpCAM-negative U87 cells (Figure 3D).^{38,39} Although all isolated clones appear to be from the same family based on upstream convergence of the lead polypeptide, four out of five of the clones tested from the matured population with DTT show a P87L/S mutation that may be beneficial for stronger binding (Figure 4). This mutation could allow for increased flexibility directly C-terminal to the engineered FG loop, enabling a more favorable conformation of the loop. Alternatively, the L/S residue itself may directly contribute as part of the binding paratope as loop-adjacent residues have been shown in the past.^{40–42} This structure–function determination is beyond the scope of this study and thus was not interrogated further.

The knowledge gained from the aforementioned experiments allows for tuning yeast-displayed cellular selections to preferentially recover higher affinity ligands in a robust, facile way without the need for decreasing target expression on the mammalian cells. This is in contrast to previous work, where fluorescein-binding scFvs were panned against RBE4 cells labeled with increasing amounts of FITC³ and EGFR-binding fibronectin domains were panned against various breast cancer cell monolayers with varying EGFR expression levels.²⁰ This is especially important for affinity maturation of engineered ligands because, after mutagenesis, it is expected that an overwhelming majority of ligands either retain or decrease their binding affinity while only a small percentage actually improve.^{43,44} The ability to modify yeast-displayed cellular selections for the enrichment of this small percentage of improved clones ensures that ligands can be selected against full-length cellular target molecules. This avoids the use of established affinity discrimination methods that use soluble extracellular domains²⁸ or detergent-solubilized cell lysates,²⁵ which may not be available or may not translate to affinity maturation against a genuine cellular target.

Additionally, though not shown in this work, the methods developed in this study could be applied directly to naïve ligand libraries for the initial rounds of selection in an attempt to isolate the highest affinity binders present in the initial pool. The success of these selections would depend on the initial library quality; ligands isolated from engineered libraries that have not yet undergone affinity maturation often have weak affinity,⁴¹ though this is not always the case.⁴⁵ In the situation

where the number of high affinity binders in the initial pool is diminishingly small, selection under conditions of reduced avidity will likely fail and is not recommended. Conversely, if a robust library is employed, then the avidity reduction approach may expedite the overall directed evolution process by enriching the high affinity binders at a much earlier round of selection.

CONCLUSIONS

In conclusion, yeast-displayed cellular selections can be modified for affinity discrimination by decreasing ligand expression with DTT treatment as ligand expression decreases titratably with increased concentration of DTT. In an EGFR model system, reducing the number of displayed ligands to 3,000–6,000 per cell allowed for 16-fold selectivity of a high-affinity (2 nM) binder relative to a mid affinity (17 nM) ligand. However, further reduction in ligand expression decreased the overall effectiveness of selection. These considerations were applied to the affinity maturation of EpCAM-binding fibronectin domains, where a small percentage of clones had a stronger target affinity than the majority of the pool but selection was not possible using standard protocols. When applied to this experimental system, cell panning selections augmented with avidity reduction enabled the isolation of novel fibronectin clones with significantly improved affinity for cellular EpCAM. These findings should ultimately increase the success of ligand engineering by aiding the isolation of strongly functional proteins that interact with full-length cellular targets.

EXPERIMENTAL PROCEDURES

Cells and Cell Culture. The MDA-MB-468 cell line was a kind gift from Professor Samira Azarin (University of Minnesota–Twin Cities). MCF-7, LnCAP, and U87 cell lines were purchased from ATCC. MDA-MB-468, MCF-7, and U87 cell lines were grown at 37 °C in a humidified atmosphere with 5% CO₂ in Dulbecco’s modified Eagle’s medium with 4.5 g/L of glucose, sodium pyruvate, and glutamine supplemented with 10% (v/v) fetal bovine serum and 1% (v/v) penicillin streptomycin. LnCAP cells were grown at 37 °C in a humidified atmosphere with 5% CO₂ in Roswell Park Memorial Institute (RPMI) medium with 4.5 g/L of glucose, sodium pyruvate, and glutamine supplemented with 10% (v/v) fetal bovine serum and 1% (v/v) penicillin streptomycin.

Yeast surface display was performed essentially as described.⁴⁶ EBY100 yeast harboring expression plasmids were grown in SD-CAA medium (16.8 g/L of sodium citrate dihydrate, 3.9 g/L of citric acid, 20.0 g/L of dextrose, 6.7 g/L of yeast nitrogen base, and 5.0 g/L of casamino acids) at 30 °C with shaking at 250 rpm. Protein expression was induced by transferring yeast cells in logarithmic phase (OD_{600 nm} < 6) into SG-CAA medium

(10.2 g/L of sodium phosphate dibasic heptahydrate, 8.6 g/L of sodium phosphate monobasic monohydrate, 19.0 g/L of galactose, 1.0 g/L of dextrose, 6.7 g/L of yeast nitrogen base, 5.0 g/L of casamino acids) and growing at 30 °C with shaking at 250 rpm for at least 8 h. EBY100 yeast without plasmid were grown in YPD medium (10.0 g/L of yeast extract, 20.0 g/L of peptone, 20.0 g/L of dextrose) at 30 °C with shaking at 250 rpm.

Expression Plasmids. The pCT-40 plasmid²⁰ was used as the expression vector for yeast surface display. This vector encodes for Aga2p followed by an 80-amino acid linker—including a factor Xa cleavage site, an HA epitope, a 40-mer linker with two repeats of the PAS#1 peptide,⁴⁷ and a glycine-rich peptide—followed by the EGFR-binding fibronectin domain E6.2.6' with a C-terminal MYC epitope. For facile analysis of clone mixtures to be enabled by flow cytometry, the MYC epitope was replaced with either a VS epitope or an E-tag epitope by elongation PCR of an arbitrary gene followed by cloning into *NheI* and *XhoI* restriction sites, yielding pCT-40V and pCT-40E, respectively. Fibronectin domain E6.2.6' N78S²⁰ was cloned into pCT-40V by *NheI* and *BamHI* restriction sites. Fibronectin domain E6.2.6' AASV²⁰ was cloned into pCT-40E by *NheI* and *BamHI* restriction sites.

Ligand Expression with DTT Titration. Yeast (5×10^6) displaying fibronectin clone E6.2.6' in the pCT-40 vector were pelleted at 8,000g and washed twice with 10 mM Tris buffer pH 7.5 (1.24 g/L of Tris-HCl, 0.26 g/L of Tris base). DTT was diluted to 0.5, 5, 10, 15, and 20 mM in 10 mM Tris buffer at pH 7.5. Yeast were resuspended in 20 μ L of DTT solution and incubated at 30 °C for 20 min without shaking. Yeast were then pelleted at 8,000g and washed twice with PBSACM (PBS with 1 g/L of bovine serum albumin, 1 mM CaCl₂, 0.5 mM MgCl₂). For relative ligand expression to be quantified, yeast were labeled with 20 μ L of anti-MYC primary antibody (9E10, BioLegend, Cat: 626802, 5 μ g/mL) for 20 min at room temperature, then washed once with PBSACM and pelleted at 8,000g for 1 min. Yeast were then labeled with 20 μ L of goat antimouse Alexa Fluor 647 conjugate (Thermo Fisher Scientific, Cat: A-21235, 10 μ g/mL) and analyzed by flow cytometry using a BD Accuri C6. The average fluorescence of 10,000 events from each sample was compared to that from an untreated control. Events with fluorescence 3 standard deviations above the mean (<3%) were omitted from this analysis.

For the absolute expression of each ligand without DTT treatment to be fully quantified, labeled yeast fluorescence was compared to a calibration curve prepared from antimouse IgG beads (Bangs Laboratories, Inc., Cat: 815). Polystyrene beads with known quantities of immobilized monoclonal antimouse IgG were labeled with 20 μ L of mouse anti-MYC antibody (9E10, BioLegend, Cat: 626802, 5 μ g/mL) and incubated for 20 min at room temperature. Beads were washed once with PBSACM and pelleted at 2,500g for 2.5 min. The beads were then labeled with 20 μ L of goat antimouse Alexa Fluor 647 conjugate (10 μ g/mL) for 20 min at room temperature. Beads were again washed with PBSACM and pelleted at 2,500g for 2.5 min. Concurrently, yeast expressing clone E6.2.6' in the pCT-40 vector were labeled equivalently with mouse anti-MYC and goat antimouse Alexa Fluor 647 conjugate as described above. Yeast expressing clone E6.2.6' in pCT-40 vector, E6.2.6' N78S in pCT-40V vector, or E6.2.6' AASV in pCT-40E vector were labeled concurrently with 20 μ L of goat anti-MYC FITC conjugate (Bethyl Laboratories, Cat: A190–104F, 2 μ g/mL), 20 μ L of goat anti-VS FITC conjugate (Bethyl Laboratories,

Cat: A190–119F, 2 μ g/mL), or 20 μ L of goat anti-E-tag FITC conjugate (Bethyl Laboratories, Cat: A190–132F, 2 μ g/mL) for 20 min at room temperature. Yeast were washed and pelleted at 8,000g for 1 min. Fluorescence was analyzed with a BD Accuri C6. The standard curve was compared to the fluorescence of the yeast that were labeled with the same mouse anti-MYC antibody and goat antimouse Alexa Fluor 647 conjugate. This expression level was mapped onto the other samples by comparison to the E6.2.6' expressing yeast labeled with the goat anti-MYC FITC conjugate.

Initial trials for yeast cell viability before and after DTT treatment were conducted using mixtures of approximately 1% pCT-40 E6.2.6', 7% pCT-40V E6.2.6' N78S, and 92% pCT-40E E6.2.6' AASV. Viability was assessed by dilution plating. Yeast (2×10^8) were pelleted at 8,000g for 1 min and washed twice with 10 mM Tris pH 7.5. As this point, viability prior to DTT treatment was assessed by dilution plating on YPD plates. Yeast were then treated with 800 μ L of 0, 2.5, 5, 10, or 15 mM DTT in Tris pH 7.5 at 30 °C for 20 min without shaking. Yeast were then pelleted at 8,000g and washed twice with PBSACM. Viability after DTT treatment was assessed by dilution plating on YPD plates. Additional trials were performed in essentially the same way except that 5×10^6 pCT-40 E6.2.6' yeast were used and the treatment volume was 20 μ L to retain the same yeast:DTT ratio.

Yeast Surface Display Cell Panning with Avidity Reduction. Yeast mixtures of approximately 1% pCT-40 E6.2.6', 7% pCT-40 V E6.2.6' N78S, and 92% pCT-40E E6.2.6' AASV were generated, and compositions were verified by flow cytometry analysis. Then, 2×10^8 yeast were washed twice with 10 mM Tris pH 7.5 and pelleted at 8,000g for 1 min. Yeast were resuspended in 800 μ L of 10 mM Tris buffer pH 7.5 with 0, 2.5, 5, 10, or 15 mM DTT, incubated at 30 °C for 20 min without shaking, washed twice with PBSACM, and pelleted at 8,000g for 1 min.

MDA-MB-468 cells were grown to approximately 80% confluence in 12-well plates. Culture medium was removed via aspiration, and cells were washed three times with 500 μ L of ice-cold PBSACM. Then, 5×10^7 yeast in 500 μ L of ice-cold PBSACM were applied to MDA-MB-468 monolayers dropwise and incubated at 4 °C without shaking for 2 h. Cells were washed five times with 500 μ L of PBSACM as described.²⁰ Briefly, cells were tilted 25 times and rotated five times for the first four washes and rotated 10 times only for the fifth wash. SD-CAA media (500 μ L) was added dropwise to each washed well, and cells were recovered by scraping. Recovered yeast were grown overnight in 5 mL of SD-CAA at 30 °C with shaking at 250 rpm, and protein expression was induced by transferring yeast into SG-CAA media and incubating for at least 8 h at 30 °C with shaking at 250 rpm. Clone composition is not expected to change due to propagation under noninduced conditions, as previously shown for this vector family.⁴⁸ Final mixture compositions were determined by flow cytometry analysis using a BD Accuri C6, as described above. Compositions, enrichment ratios, and selectivities are reported as mean \pm standard deviation of eight selections.

Affinity Selection of EpCAM-Binding Engineered Fibronectin Domains. EpCAM-binding fibronectin domains were selected via yeast surface display essentially as described.⁴⁶ Details regarding yeast cell growth and induction of ligand surface display are given above. Briefly, a yeast-display library of fibronectin domains⁴⁵ was subjected to negative selection against avidin-coated magnetic beads followed by magnetic beads

functionalized with irrelevant protein lysozyme to remove any nonspecific binding interactions. Remaining yeast were then exposed to magnetic beads functionalized with biotinylated recombinant human EpCAM (Acro Biosystems, Cat: EPM-H8223), and bound yeast were selected. Incubations were performed at 4 °C, and recovered beads were washed once in PBSA (PBS with 1 g/L of bovine serum albumin) prior to culture in SD-CAA media at 30 °C at 250 rpm for at least 12 h. Protein induction was then induced as described above.

After three rounds of magnetic selection, full-length (MYC-positive) fibronectin clones were selected via FACS using mouse anti-MYC antibody (9E10, BioLegend, Cat: 626802, 5 µg/mL) and goat antimouse Alexa Fluor 647 conjugate (Thermo Fisher Scientific, Cat: A-21235, 10 µg/mL). Isolated clones were subject to whole-gene and loop-focused error-prone PCR using mutagenic nucleotide analogues⁴⁹ and genetic loop shuffling between sequences.⁴¹ After transformation of the mutants into EBY100 yeast, the resulting population was subjected to one additional round of magnetic selection at 4 °C; recovered beads were washed twice with PBSA prior to culture in SD-CAA media at 30 °C at 250 rpm for at least 12 h. Ligand expression was induced as above. Yeast were then subjected to two rounds of mammalian cell selection against adherent monolayers of the EpCAM-overexpressing cell lines MCF-7 and LNCaP (Figure S1), as previously described.²⁰ Full length clones that bound biotinylated target, detected with a streptavidin Alexa Fluor 488 conjugate (Thermo Fisher Scientific, Cat: S-11223, 10 µg/mL), were then isolated via FACS and diversified as before.

After three additional rounds of panning against MCF-7 and LNCaP cell lines, target binding yeast were again isolated by FACS and diversified before panning against the same cell lines once more. This population was then subjected to three rounds of cell panning against MCF-7 cells in two parallel strategies: via the standard approach outlined above or with yeast valency reduction. In the case of the standard approach, yeast were panned against MCF-7 cells without DTT treatment. For yeast valency reduction, yeast were treated with 2.5, 5, 7, and 9 mM DTT and washed as previously described. Valency was assessed by flow cytometry analysis with fluorescence standard beads and as previously described. The DTT treatment yielding a population with between 3,000 and 6,000 ligands per yeast cell (often 2.5–5 mM, depending on the untreated level of protein expression) was used for selection.

Protein Production and Analysis. BL21(DE3) *Escherichia coli* (New England Biolabs, Cat: C25661) were transformed with plasmid and grown overnight (37 °C, 250 rpm) in lysogeny broth (LB) medium with kanamycin (50 µg/mL). Approximately 4 mL of overnight culture was added to 100 mL of LB medium without antibiotics and grown at 37 °C at 250 rpm until the optical density at 600 nm (OD₆₀₀) reached 0.65–1.0 (~2 h) and induced with 1.0 mM isopropyl β-D-1-thiogalactopyranoside (IPTG) for 3 h at 30 °C and 250 rpm. Cells were pelleted (3,500g, 15 min, 4 °C), frozen in a dry ice/ethanol bath, and resuspended in 8 mL of SoluLyse protein extraction reagent (Genlantis Inc., Cat: L100125) supplemented with EDTA-free protease inhibitor (Thermo Fisher Scientific, Cat: 88266). Cell lysates were centrifuged (27,000g, 15 min, 4 °C) to separate soluble and insoluble protein fractions, and the supernatant was filtered through a 0.22 µm membrane. Fibronectin domains were purified by immobilized metal affinity chromatography on a gravity column packed with HisPur cobalt resin (Thermo Fisher Scientific, Cat: 89964)

following the manufacturer's protocol, and eluted fractions were analyzed by SDS-PAGE. Fractions containing visibly pure fibronectin domains were pooled and buffer exchanged into phosphate buffered saline (PBS), pH 7.4, with Zeba spin desalting columns (Thermo Fisher Scientific, Cat: 89893). Protein concentration was determined via Bradford Protein Assay (Bio-Rad Laboratories, Cat: 500–0201) and diluted to 1 µM in additional PBS. Purified protein was analyzed by size-exclusion chromatography (SEC) on a Superdex 200 Increase 10/300 gel filtration column (GE Healthcare Life Sciences, Cat: 28990944) in PBS running buffer. Retention times of fibronectin domains were compared to those of commercial molecular weight standards (Sigma-Aldrich, Cat: C7150 and C7025, respectively) cytochrome C (14.6 kDa) and carbonic anhydrase (29 kDa) and found to be ≥80% monomeric (Figures S4 and S5).

Affinity Determination of Fibronectin Domains. MCF-7 cells were cultured to approximately 80% confluence, as described above. Detached MCF-7 cells were counted using a Countess II Automated Cell Counter. Aliquots of 40,000 MCF-7 cells were washed and labeled with varying concentrations of each fibronectin clone for 90 min at 4 °C with rotation. Cells were pelleted at 300g for 3 min, washed with 1 mL of ice-cold PBSACM, and labeled with 20 µL of anti-His₆ FITC conjugate (Abcam, Cat: ab1206, 13 µg/mL) for 20 min at 4 °C in the dark. Cells were again pelleted and washed with 1 mL of ice-cold PBSACM. Fluorescence was analyzed using a BD Accuri C6 or BD LSRII.

■ ASSOCIATED CONTENT

● Supporting Information

The Supporting Information is available free of charge on the ACS Publications website at DOI: 10.1021/acscmbosci.6b00191.

EpCAM expression of MCF-7 and LNCaP mammalian cell lines, SEC characterizations for soluble protein domains, affinity estimations for intermediate anti-EpCAM fibronectin clones, comparison of soluble anti-EpCAM fibronectin clones to a monoclonal antibody positive control, and associated materials and methods (PDF)

■ AUTHOR INFORMATION

Corresponding Author

*E-mail: hackel@umn.edu. Phone: 612-624-7102. Fax: 612-626-7246.

ORCID

Carston R. Wagner: 0000-0001-7927-719X

Benjamin J. Hackel: 0000-0003-3561-9463

Funding

This work was funded by the National Institutes of Health R21 EB019518 (BJH), R21 CA185627 (CRW), F30 CA210345 (CMC), and the University of Minnesota.

Notes

The authors declare no competing financial interest.

■ REFERENCES

- (1) Leader, B.; Baca, Q. J.; Golan, D. E. Protein Therapeutics: A Summary and Pharmacological Classification. *Nat. Rev. Drug Discovery* **2008**, 7 (1), 21–39.
- (2) James, M. L.; Gambhir, S. S. A Molecular Imaging Primer: Modalities, Imaging Agents, and Applications. *Physiol. Rev.* **2012**, 92 (2), 897–965.

- (3) Wang, X. X.; Shusta, E. V. The Use of scFv-Displaying Yeast in Mammalian Cell Surface Selections. *J. Immunol. Methods* **2005**, *304* (1–2), 30–42.
- (4) Tillotson, B. J.; Cho, Y. K.; Shusta, E. V. Cells and Cell Lysates: A Direct Approach for Engineering Antibodies against Membrane Proteins Using Yeast Surface Display. *Methods* **2013**, *60* (1), 27–37.
- (5) Wang, X. X.; Cho, Y. K.; Shusta, E. V. Mining a Yeast Library for Brain Endothelial Cell-Binding Antibodies. *Nat. Methods* **2007**, *4* (2), 143–145.
- (6) Dangaj, D.; Lanitis, E.; Zhao, A.; Joshi, S.; Cheng, Y.; Sandaltzopoulos, R.; Ra, H. J.; Danet-Desnoyers, G.; Powell, D. J.; Scholler, N. Novel Recombinant Human B7-H4 Antibodies Overcome Tumoral Immune Escape to Potentiate T-Cell Antitumor Responses. *Cancer Res.* **2013**, *73* (15), 4820–4829.
- (7) Williams, R. M.; Hajiran, C. J.; Nayeem, S.; Sooter, L. J. Identification of an Antibody Fragment Specific for Androgen-Dependent Prostate Cancer Cells. *BMC Biotechnol.* **2014**, *14* (1), 81.
- (8) Ackerman, M.; Levary, D.; Tobon, G.; Hackel, B.; Orcutt, K. D.; Wittrup, K. D. Highly Avid Magnetic Bead Capture: An Efficient Selection Method for de Novo Protein Engineering Utilizing Yeast Surface Display. *Biotechnol. Prog.* **2009**, *25* (3), 774–783.
- (9) McCafferty, J.; Griffiths, A. D.; Winter, G.; Chiswell, D. J. Phage Antibodies: Filamentous Phage Displaying Antibody Variable Domains. *Nature* **1990**, *348* (6301), 552–554.
- (10) Boder, E. T.; Wittrup, K. D. Yeast Surface Display for Screening Combinatorial Polypeptide Libraries. *Nat. Biotechnol.* **1997**, *15*, 553–557.
- (11) Baneyx, F.; Mujacic, M. Recombinant Protein Folding and Misfolding in *Escherichia Coli*. *Nat. Biotechnol.* **2004**, *22* (11), 1399–1408.
- (12) Gasser, B.; Saloheimo, M.; Rinas, U.; Dragosits, M.; Rodríguez-Carmona, E.; Baumann, K.; Giuliani, M.; Parrilli, E.; Branduardi, P.; Lang, C.; Porro, D.; Ferrer, P.; Tutino, M.; Mattanovich, D.; Villaverde, A. Protein Folding and Conformational Stress in Microbial Cells Producing Recombinant Proteins: A Host Comparative Overview. *Microb. Cell Fact.* **2008**, *7* (1), 11.
- (13) Mazzei, G. J.; Edgerton, M. D.; Losberger, C.; Lecoanet-Henchoz, S.; Graber, P.; Durandy, A.; Gauchat, J. F.; Bernard, A.; Allet, B.; Bonnefoy, J. Y. Recombinant Soluble Trimeric CD40 Ligand Is Biologically Active. *J. Biol. Chem.* **1995**, *270*, 7025–7028.
- (14) Singer, E.; Landgraf, R.; Horan, T.; Slamon, D.; Eisenberg, D. Identification of a Heregulin Binding Site in HER3 Extracellular Domain. *J. Biol. Chem.* **2001**, *276* (47), 44266–44274.
- (15) Gomord, V.; Faye, L. Posttranslational Modification of Therapeutic Proteins in Plants. *Curr. Opin. Plant Biol.* **2004**, *7* (2), 171–181.
- (16) Demain, A. L.; Vaishnav, P. Production of Recombinant Proteins by Microbes and Higher Organisms. *Biotechnol. Adv.* **2009**, *27*, 297–306.
- (17) Kruziki, M. A.; Bhatnagar, S.; Woldring, D. R.; Duong, V. T.; Hackel, B. J. A 45-Amino-Acid Scaffold Mined from the PDB for High-Affinity Ligand Engineering. *Chem. Biol.* **2015**, *22*, 1–11.
- (18) Li, J.; Lundberg, E.; Vernet, E.; Larsson, B.; Höiden-Guthenberg, I.; Gräslund, T. Selection of Affibody Molecules to the Ligand-Binding Site of the Insulin-like Growth Factor-1 Receptor. *Biotechnol. Appl. Biochem.* **2010**, *55* (2), 99–109.
- (19) Friedman, M.; Nordberg, E.; Höiden-Guthenberg, I.; Brismar, H.; Adams, G. P.; Nilsson, F. Y.; Carlsson, J.; Ståhl, S. Phage Display Selection of Affibody Molecules with Specific Binding to the Extracellular Domain of the Epidermal Growth Factor Receptor. *Protein Eng., Des. Sel.* **2007**, *20* (4), 189–199.
- (20) Stern, L. A.; Schrack, I. A.; Johnson, S. M.; Deshpande, A.; Bennett, N. R.; Harasymiw, L. A.; Gardner, M. K.; Hackel, B. J. Geometry and Expression Enhance Enrichment of Functional Yeast-Displayed Ligands via Cell Panning. *Biotechnol. Bioeng.* **2013**, *113* (11), 2328–2341.
- (21) Joyce, G. F. Directed Molecular Evolution. *Sci. Am.* **1992**, *267* (6), 90–97.
- (22) Beaudry, A. A.; Joyce, G. F. Directed Evolution of an RNA Enzyme. *Science* **1992**, *257* (5070), 635–641.
- (23) Chen, K.; Arnold, F. H. Tuning the Activity of an Enzyme for Unusual Environments: Sequential Random Mutagenesis of Subtilisin E for Catalysis in Dimethylformamide. *Proc. Natl. Acad. Sci. U. S. A.* **1993**, *90* (12), 5618–5622.
- (24) Stemmer, W. P. C. Rapid Evolution of a Protein in Vitro by DNA Shuffling. *Nature* **1994**, *370* (6488), 389–391.
- (25) Cho, Y. K.; Shusta, E. V. Antibody Library Screens Using Detergent-Solubilized Mammalian Cell Lysates as Antigen Sources. *Protein Eng., Des. Sel.* **2010**, *23* (7), 567–577.
- (26) Tillotson, B. J.; De Larrinoa, I. F.; Skinner, C. A.; Klavas, D. M.; Shusta, E. V. Antibody Affinity Maturation Using Yeast Display with Detergent-Solubilized Membrane Proteins as Antigen Sources. *Protein Eng., Des. Sel.* **2013**, *26* (2), 101–112.
- (27) Schmidt, M. M.; Wittrup, K. D. A Modeling Analysis of the Effects of Molecular Size and Binding Affinity on Tumor Targeting. *Mol. Cancer Ther.* **2009**, *8* (10), 2861–2871.
- (28) VanAntwerp, J. J.; Wittrup, K. D. Fine Affinity Discrimination by Yeast Surface Display and Flow Cytometry. *Biotechnol. Prog.* **2000**, *16* (1), 31–37.
- (29) Föllmann, W.; Wober, J. Investigation of Cytotoxic, Genotoxic, Mutagenic, and Estrogenic Effects of the Flame Retardants Tris-(2-Chloroethyl)-Phosphate (TCEP) and Tris-(2-Chloropropyl)-Phosphate (TCPP) in Vitro. *Toxicol. Lett.* **2006**, *161* (2), 124–134.
- (30) Went, P. T.; Lugli, A.; Meier, S.; Bundi, M.; Mirlacher, M.; Sauter, G.; Dirnhofer, S. Frequent EpCam Protein Expression in Human Carcinomas. *Hum. Pathol.* **2004**, *35* (1), 122–128.
- (31) Eder, M.; Knackmuss, S.; Le Gall, F.; Reusch, U.; Rybin, V.; Little, M.; Haberkorn, U.; Mier, W.; Eisenhut, M. 68Ga-Labelled Recombinant Antibody Variants for Immuno-PET Imaging of Solid Tumours. *Eur. J. Nucl. Med. Mol. Imaging* **2010**, *37* (7), 1397–1407.
- (32) Zielonka, S.; Weber, N.; Becker, S.; Doerner, A.; Christmann, A.; Christmann, C.; Uth, C.; Fritz, J.; Schäfer, E.; Steinmann, B.; Empting, M.; Ockelmann, P.; Lierz, M.; Kolmar, H. Shark Attack: High Affinity Binding Proteins Derived from Shark vNAR Domains by Stepwise in Vitro Affinity Maturation. *J. Biotechnol.* **2014**, *191*, 236–245.
- (33) Martin-Killias, P.; Patricia, M.-K.; Stefan, N.; Rothschild, S.; Plückthun, A.; Zangemeister-Wittke, U. A Novel Fusion Toxin Derived from an EpCAM-Specific Designed Ankyrin Repeat Protein Has Potent Antitumor Activity. *Clin. Cancer Res.* **2011**, *17* (1), 100–110.
- (34) Stefan, N.; Martin-Killias, P.; Wyss-Stoeckle, S.; Honegger, A.; Zangemeister-Wittke, U.; Plückthun, A. DARPins Recognizing the Tumor-Associated Antigen EpCAM Selected by Phage and Ribosome Display and Engineered for Multivalency. *J. Mol. Biol.* **2011**, *413* (4), 826–843.
- (35) Iwasaki, K.; Goto, Y.; Katoh, T.; Yamashita, T.; Kaneko, S.; Suga, H. A Fluorescent Imaging Probe Based on a Macrocyclic Scaffold That Binds to Cellular EpCAM. *J. Mol. Evol.* **2015**, *81* (5–6), 210–217.
- (36) Koide, A.; Bailey, C. W.; Huang, X.; Koide, S. The Fibronectin Type III Domain as a Scaffold for Novel Binding Proteins. *J. Mol. Biol.* **1998**, *284* (4), 1141–1151.
- (37) Lipovšek, D. Adnectins: Engineered Target-Binding Protein Therapeutics. *Protein Eng., Des. Sel.* **2011**, *24* (1–2), 3–9.
- (38) Shibata, T.; Uchida, H.; Shiroyama, T.; Okubo, Y.; Suzuki, T.; Ikeda, H.; Yamaguchi, M.; Miyagawa, Y.; Fukuhara, T.; Cohen, J. B.; Glorioso, J. C.; Watabe, T.; Hamada, H.; Tahara, H. Development of an Oncolytic HSV Vector Fully Retargeted Specifically to Cellular EpCAM for Virus Entry and Cell-to-Cell Spread. *Gene Ther.* **2016**, *23* (6), 479–488.
- (39) MacArthur, K. M.; Kao, G. D.; Chandrasekaran, S.; Alonso-Basanta, M.; Chapman, C.; Lustig, R. A.; Wileyto, E. P.; Hahn, S. M.; Dorsey, J. F. Detection of Brain Tumor Cells in the Peripheral Blood by a Telomerase Promoter-Based Assay. *Cancer Res.* **2014**, *74* (8), 2152–2159.

- (40) Porebski, B. T.; Conroy, P. J.; Drinkwater, N.; Schofield, P.; Vazquez-Lombardi, R.; Hunter, M. R.; Hoke, D. E.; Christ, D.; McGowan, S.; Buckle, A. M. Circumventing the Stability-Function Trade-off in an Engineered FN3 Domain. *Protein Eng., Des. Sel.* **2016**, *29* (11), 541–550.
- (41) Hackel, B. J.; Kapila, A.; Wittrup, K. D. Picomolar Affinity Fibronectin Domains Engineered Utilizing Loop Length Diversity, Recursive Mutagenesis, and Loop Shuffling. *J. Mol. Biol.* **2008**, *381* (5), 1238–1252.
- (42) Koide, A.; Wojcik, J.; Gilbreth, R. N.; Hoey, R. J.; Koide, S. Teaching an Old Scaffold New Tricks: Monobodies Constructed Using Alternative Surfaces of the FN3 Scaffold. *J. Mol. Biol.* **2012**, *415* (2), 393–405.
- (43) Tokuriki, N.; Stricher, F.; Schymkowitz, J.; Serrano, L.; Tawfik, D. S. The Stability Effects of Protein Mutations Appear to Be Universally Distributed. *J. Mol. Biol.* **2007**, *369* (5), 1318–1332.
- (44) Daugherty, P. S.; Chen, G.; Iverson, B. L.; Georgiou, G. Quantitative Analysis of the Effect of the Mutation Frequency on the Affinity Maturation of Single Chain Fv Antibodies. *Proc. Natl. Acad. Sci. U. S. A.* **2000**, *97* (5), 2029–2034.
- (45) Woldring, D. R.; Holec, P. V.; Zhou, H.; Hackel, B. J. High-Throughput Ligand Discovery Reveals a Sitewise Gradient of Diversity in Broadly Evolved Hydrophilic Fibronectin Domains. *PLoS One* **2015**, *10* (9), e0138956.
- (46) Chen, T. F.; de Picciotto, S.; Hackel, B. J.; Wittrup, K. D. Engineering Fibronectin-Based Binding Proteins by Yeast Surface Display. *Methods Enzymol.* **2013**, *523*, 303–326.
- (47) Schlapschy, M.; Binder, U.; Börger, C.; Theobald, I.; Wachinger, K.; Kisling, S.; Haller, D.; Skerra, A. PASylation: A Biological Alternative to PEGylation for Extending the Plasma Half-Life of Pharmaceutically Active Proteins. *Protein Eng., Des. Sel.* **2013**, *26*, 489–501.
- (48) Feldhaus, M. J.; Siegel, R. W.; Opresko, L. K.; Coleman, J. R.; Feldhaus, J. M.; Yeung, Y. A.; Cochran, J. R.; Heinzelman, P.; Colby, D.; Swers, J.; Graff, C.; Wiley, H. S.; Wittrup, K. D. Flow-Cytometric Isolation of Human Antibodies from a Nonimmune *Saccharomyces Cerevisiae* Surface Display Library. *Nat. Biotechnol.* **2003**, *21* (2), 163–70.
- (49) Zaccolo, M.; Williams, D. M.; Brown, D. M.; Gherardi, E. An Approach to Random Mutagenesis of DNA Using Mixtures of Triphosphate Derivatives of Nucleoside Analogues. *J. Mol. Biol.* **1996**, *255* (4), 589–603.